NeuroImage 208 (2020) 116463

Contents lists available at ScienceDirect

NeuroImage

journal homepage: www.elsevier.com/locate/neuroimage

Sub-millimeter fMRI reveals multiple topographical digit representations that form action maps in human motor cortex

Laurentius Huber (Renzo) [a,b,*], Emily S. Finn [a], Daniel A. Handwerker [a], Marlene Bönstrup [c,d], Daniel R. Glen [a], Sriranga Kashyap [b], Dimo Ivanov [b], Natalia Petridou [e], Sean Marrett [a], Jozien Goense [f], Benedikt A. Poser [b], Peter A. Bandettini [a]

[a] NIMH, NIH, Bethesda, MD, USA
[b] Maastricht Brain Imaging Centre, Maastricht University, Maastricht, the Netherlands
[c] NINDS, NIH, Bethesda, MD, USA
[d] Department of Neurology, University of Leipzig, Leipzig, Germany
[e] University Medical Center Utrecht, Center for Image Sciences, Utrecht, the Netherlands
[f] School of Psychology, Institute of Neuroscience and Psychology, University of Glasgow, Glasgow, UK

ARTICLE INFO

Keywords:
fMRI
Motor cortex
Cortical layers
Cortical columns
VASO

ABSTRACT

The human brain coordinates a wide variety of motor activities. On a large scale, the cortical motor system is topographically organized such that neighboring body parts are represented by neighboring brain areas. This homunculus-like somatotopic organization along the central sulcus has been observed using neuroimaging for large body parts such as the face, hands and feet. However, on a finer scale, invasive electrical stimulation studies show deviations from this somatotopic organization that suggest an organizing principle based on motor actions rather than body part moved. It has not been clear how the action-map organization principle of the motor cortex in the mesoscopic (sub-millimeter) regime integrates into a body map organization principle on a macroscopic scale (cm). Here we developed and applied advanced mesoscopic (sub-millimeter) fMRI and analysis methodology to non-invasively investigate the functional organization topography across columnar and laminar structures in humans. Compared to previous methods, in this study, we could capture locally specific blood volume changes across entire brain regions along the cortical curvature. We find that individual fingers have multiple mirrored representations in the primary motor cortex depending on the movements they are involved in. We find that individual digits have cortical representations up to 3 mm apart from each other arranged in a column-like fashion. These representations are differentially engaged depending on whether the digits' muscles are used for different motor actions such as flexion movements, like grasping a ball or retraction movements like releasing a ball. This research provides a starting point for non-invasive investigation of mesoscale topography across layers and columns of the human cortex and bridges the gap between invasive electrophysiological investigations and large coverage non-invasive neuroimaging.

1. Introduction

The human repertoire of motor activity spans an immense variety of movements, and most of our interactions with the environment involve some degree of movement. Voluntary movement is controlled by the central nervous system, particularly the brain's motor cortex. The primary motor cortex is organized according to the principle of somatotopy, whereby areas controlling different body parts are arranged in a predictable order. Penfield and colleagues (Penfield and Boldrey, 1937) were the first to report the medial-to-lateral leg-to-face somatotopic "homunculus" in the human primary motor cortex; a representation that has been confirmed with neuroimaging for large body parts (Schieber 2002; Chainay et al., 2004) and digits (Siero et al., 2014; Olman et al., 2012; Schellekens et al., 2018) in the spatial regime of centimeters. However, fundamental deviations from this simple linear arrangement of body parts have been reported at a more microscopic level (Penfield and Boldrey, 1937; Barinaga, 1995; Strother et al., 2012; Scheiber and Hibbard, 1993; Strick and Preston, 1982; Sanes et al., 1995; Meier et al.,

* Corresponding author. NIMH, NIH, Bethesda, MD, USA.
E-mail address: renzohuber@gmail.com (L. Huber).

https://doi.org/10.1016/j.neuroimage.2019.116463
Received 6 June 2019; Received in revised form 10 November 2019; Accepted 11 December 2019
Available online 17 December 2019

2008; Indovina and Sanes, 2001; Hlustik et al., 2001; Lemon, 1988). As such, the neuronal representations of individual body parts show a large gradual overlap in the same location of the cortex (Schieber 2002; Scheiber and Hibbard, 1993; Indovina and Sanes, 2001). And also, the progression of body part representations along the cortical ribbon from face towards leg does not follow a corresponding simple linear arrangement. Instead, multiple unconnected body part representations were reported, in rhesus macaque monkeys (Park et al., 2001). And it was suggested that the hand is emphasized in a core region, and the wrist, arm, and shoulder are emphasized in a half ring surrounding the core (Strother et al., 2012; Strick and Preston, 1982; Porter and Lemon, 1993; Kwan et al., 1978).

In light of these deviations from a linear somatotopic organization, alternative organizational principles for the motor cortex have been investigated. Previous findings show that when a small part in the monkey motor cortex is electrically stimulated, the resulting movement combines joints and muscles in a manner resembling a coordinated action (Graziano et al., 2002), suggesting that the motor cortex organization might follow an action map representation rather than a body part map (Sanes et al., 1995; Graziano, 2016; Graziano and Aflalo, 2007a). More recently, Diedrichsen and colleagues. also found fMRI evidence, which confirms that large portions of the motor cortex represent complex muscle synergies in humans too (Ejaz et al., 2015).

The body map organization and the action map organization may seem like they are *competing* with each other. However, they do not necessarily need to be mutually exclusive. Graziano and Aflalo (2007a; 2007b) came up with a well developed model of how an action map and a somatotopic map may co-exist in the same cortical space (Graziano and Aflalo, 2007b). This integration principle is analogous to the organization of V1 with its large-scale map of the retina and small-scale map of orientation columns. In the view of the motor cortex, the large-scale map is shaped by somatotopic principles, and at the smaller scale the map is re-organized around actions. Here, we aim to investigate this integration principle in the human motor cortex. Until now, it is not clear at which spatial scale the somatotopic body map representation breaks down in humans and how it is represented across cortical depth.

Due to recent methodological advances in fMRI (Polimeni et al., 2010; De Martino et al., 2015; Huber et al., 2017) the mesoscopic regime of sub-millimeter resolutions becomes accessible for non-invasive functional neuroimaging across the columnar and laminar scale in humans. Thus, mesoscopic fMRI could provide insights on how (microscopic) action maps are integrated into (macroscopic) somatotopical body part maps. However, these existing mesoscopic fMR methods can only capture small patches of cortex with thick slices and without the ability to resolve columnar structures and laminar structures simultaneously. Therefore, they do not allow the investigation of microscale topographic movement representations in humans.

This study develops advanced high-resolution imaging methods and novel analysis methodology to investigate topographical organization patterns across the 'columnar' and 'laminar' cortical dimensions with CBV-senitive fMRI across large patches of cortex. Note, that in the context of fMRI, 'columnar' and 'laminar' refer to mesoscopic structures that are aligned along (tangential) and perpendicular (radial) to the cortical depths (a.k.a. 'cortical depths' and 'hypercolumns'). The method improvements could be achieved with conventional 7T MRI hardware and a non-invasive VASO (vascular space occupancy) sequence (Lu et al., 2003; Hua et al., 2013; Huber et al., 2014a). We investigated the neuroscientific applicability of the new methodology by mapping the meso-scale (sub-millimeter) topographical representations of the primary motor (M1) and primary sensory cortex (S1; the posterior bank of the central sulcus). We use this approach to investigate the organizational principle of individual finger representations for a set of simple motor actions including tapping, grasping (flexion) and retraction movements (extension). We find mesoscopic topographic finger representations in M1 (BA4a) on the order of 1.2 ± 0.4 mm. We also find evidence of a simple topographical organizational principle: Fingers are represented in multiple somatotopically organized patches that are preferentially activated for either grasping or retraction movement actions.

2. Methods in brief

Five participants underwent 84 h of scanning at 7T with SS-SI-VASO (Huber et al., 2014a) at a resolution of 0.79 × 0.79 × 0.99 mm^3. To investigate the columnar organization of the primary motor cortex with fMRI, five different experiments (Fig. S1) were conducted. These were:

A Individual tapping of two fingers (index and little).
B Individual tapping of four fingers (index, middle, ring, and little; no thumb) interspaced with rest periods.
C Individual tapping of all five fingers (index, middle, ring, little, and thumb) interspaced with rest periods.
D Alternating grasping or retraction of a rubber ball interspaced with rest periods. These tasks engage muscle extension and muscle flexion of every finger.
E Resting-state.

Motor tasks were performed with the left hand, while imaging the primary sensorimotor cortex on both sides of the central sulcus in the right hemisphere (Fig. 1A). The right hand was not engaged during any of experiments of this study. For more background on these tasks and explanations, why this task setup was used, see the supplementary information (Fig. S1). Five participants underwent 42 fMRI total sessions of 2 h each (84h of scanning, Table S1). We simultaneously measured changes in the cerebral blood volume (CBV) and blood oxygenation level dependent (BOLD) response using the SS-SI-VASO method (Lu et al., 2003; Huber et al., 2014a) with a 3D-EPI readout (Poser et al., 2010) at 7T. The nominal resolution was 0.79 mm in the columnar dimension and 0.99 mm thick slices perpendicular to the precentral bank of the central sulcus – also known as the hand knob (Fig. 1A). Estimates of cortical depths (layers) and cortical distances (columns) across the entire central sulcus were calculated by means of simultaneously acquired anatomical and functional image contrasts in EPI space (Fig. 1B). Details on the data acquisition and analysis approach are provided in the Detailed Experimental Procedures (Figs. S1–S10). The functional percent signal changes were calculated as $100\times(Sactivity - Srest)/Srest$ (see also Fig. S2 left columns of panels respectively). For relative finger dominance analysis, we estimated the finger selectivity as:

$$S^i_{dminance} = \frac{S^i_{activity}}{\sum_{remaining\ fingers} S^i_{activity}} \quad (1)$$

with $i\{thumb, index, middle, ring, little\}$, while $S^i_{activity}$ refers to the above percent signal change (see also middle column in panels of Fig. S2). The grasping and retraction reference was calculated as 100 x $(S_{grasping} - S_{retraction})/S_{rest}$ and 100 x $(S_{retraction} - S_{grasping})/S_{rest}$, respectively.

3. Results

Functional MRI signal changes in S1 show a linear arrangement of individual digits (Fig. 1) as previously described in high-resolution fMRI studies (Siero et al., 2014; Olman et al., 2012; Ejaz et al., 2015; Sanchez Panchuelo et al., 2016; Kolasinski et al., 2016; Schluppeck et al., 2018). The distance between the representations of the thumb and the little finger in S1 is 16 ± 4 mm. In M1, we find clear deviations from a continuous linear arrangement of the digit representations; we find multiple representations of every digit in a mirrored pattern (Fig. 2). These digit representations are significantly smaller than the representations in the sensory cortex. The distance between the representations of the thumb and the little finger in M1 is 6 ± 2 mm. The mirrored pattern of multiple distant digit representations was highly consistent across

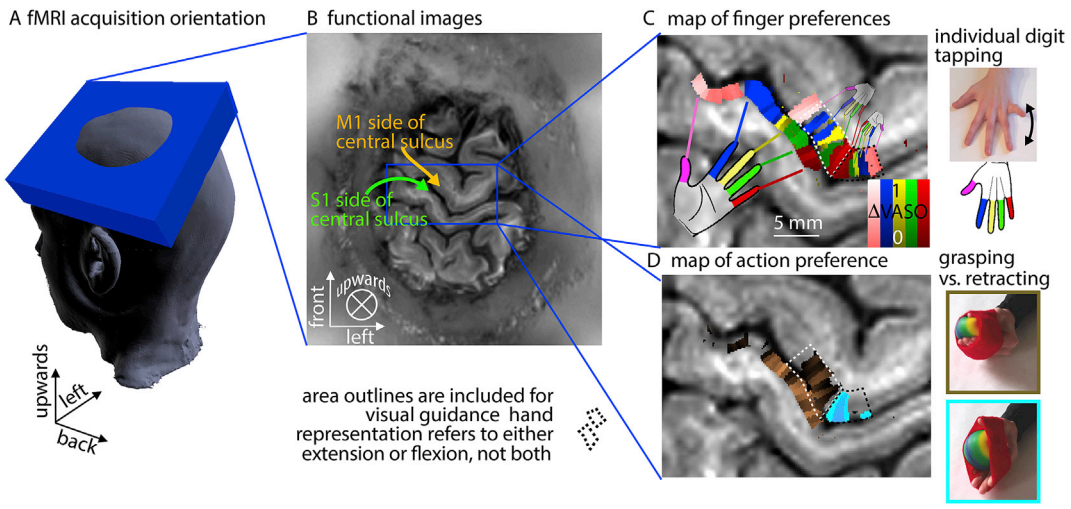

Fig. 1. Acquisition and analysis methods for measuring the laminar and columnar functional topography. A-B) The imaging slab is aligned to cover the entire primary sensorimotor cortex and slices are tilted as indicated by the blue box through the right cortical hemisphere. C) The functional CBV signal changes obtained using a five-finger tapping task reveal individual digit representations in M1 and S1. While S1 has a homunculus like linear representation of individual digits, the primary motor cortex shows clear deviations of the homunculus model. D) While S1 has a stronger activity for grasping compared to retraction motor actions, the primary motor cortex shows individual patches of areas that are either specific to grasping or retraction actions. For further graphical guidance about the respective dimensions and coordinate systems, see Fig. S3. All functional results shown here refer to left hand movement tasks. The right hand was not engaged here.

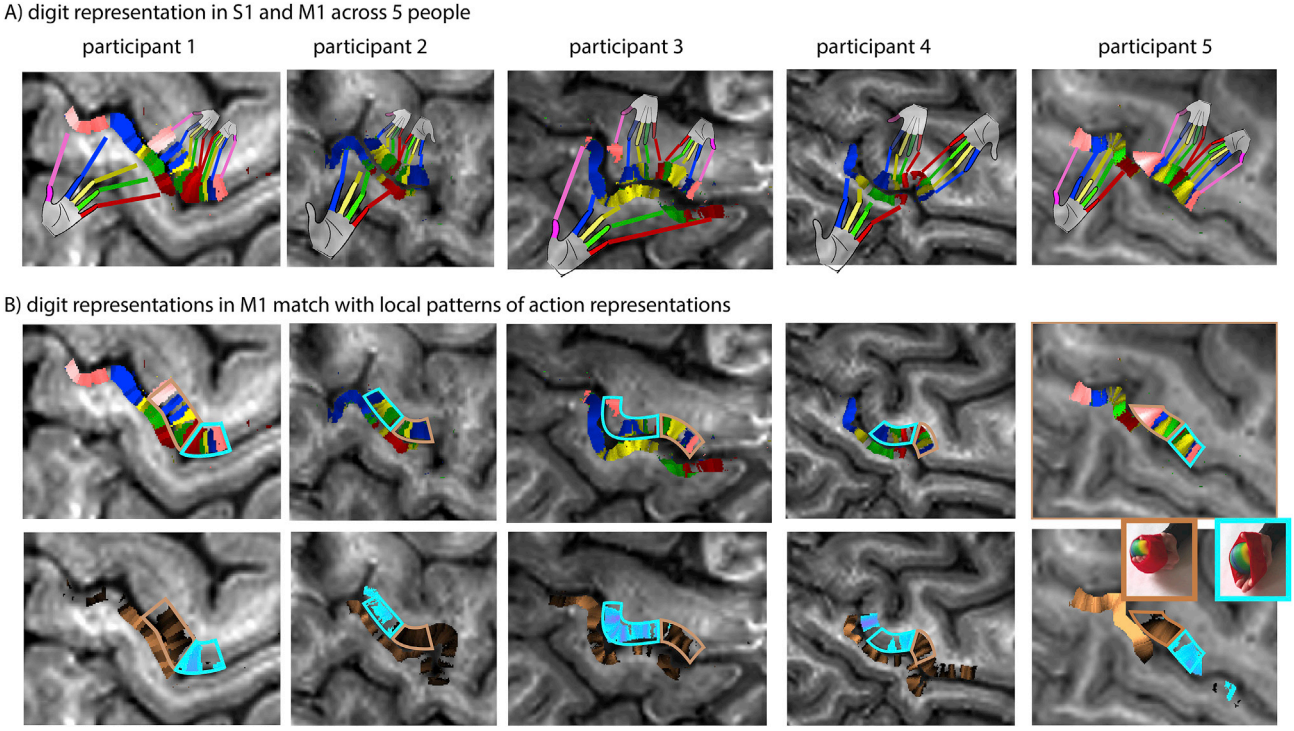

Fig. 2. Multiple hand representations across participants. A) The finger dominance maps show across all participants that the primary sensory cortex has a single representation of each finger in all participants, while the primary motor cortex has multiple finger representations of each finger. The representations in the primary motor cortex are mirrored and about half the size of the representations in the primary somatosensory cortex. B) The spatial pattern of multiple finger representations is compared to the representations of different movements, grasping and retraction of a ball. Each complete set of fingers is outlined with manually drawn borders. These borders match the outlines of the different action tasks. The copper and turquoise colors refer to preferred grasping and retraction preference, respectively. The functional contrast refers to relative action preference between task conditions. I.e., turquoise patches refer to stronger activity during retraction periods compared to grasping periods (see also Fig. S7 for absolute signal changes). The maps in the left column are the same as in Fig. 1. All functional results shown here refer to CBV changes during left hand movement tasks. The right hand was not engaged.

participants (Fig. 2), across fMRI contrasts (Fig. S5), and across days (Fig. S6).

We find that different patches of the hand knob in M1 are preferentially activated during grasping and retraction movements, respectively. These patches are 6 ± 2 mm in size and columnar distance. We find that the outlines of grasping and retraction preference patches contain complete sets of all digit preferences (copper and turquoise outlines in Fig. 2B).

We next quantified relative preferences for body parts (i.e., different fingers) and movements (i.e., grasping versus retraction) along the

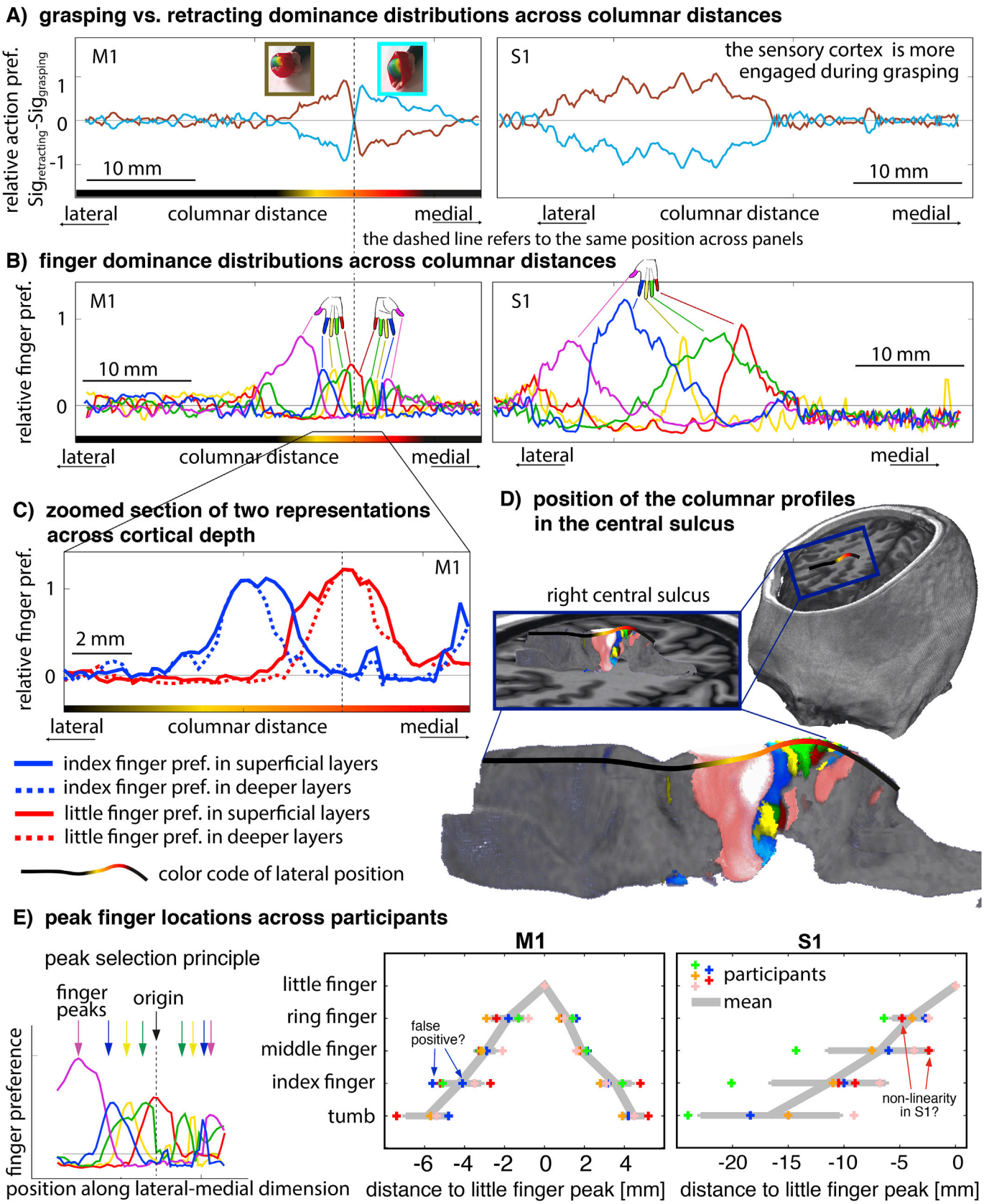

(caption on next page)

Fig. 3. Columnar profiles of functional representations along the central sulcus of participant 1. Panel A) depicts the columnar distribution of grasping preference and retraction preference. While the entire primary sensory cortex is more engaged for grasping actions, the primary motor cortex has distinct patches that are preferentially more active for either grasping or retraction. Panel B) shows that each of the patches in the primary motor cortex contains a complete set of linearly aligned finger patches. Panel C) shows that superficial cortical layers have larger overlap across fingers compared to deeper layers. The dashed line in panel A–C refers to the same columnar position. The unit of the y-axis refers to the relative signal change between conditions (see Fig. S5). The results refer to a projection of a 0.79 mm slab through the central sulcus (D). The scale bars refer to the spatial distance along the curved GM accounting for the average curvature in the projection slab. The anatomical contrast along these columnar profiles is given in Fig. S7 for reference. To depict the double finger representation clearer in a more quantitative fashion across participants, we plot the peaks of the columnar profiles in panel E) along the following procedure. First, the peak of the little finger preference is selected and used as the origin of the coordinate system. Then each fingers peaks of relative preferences are extracted for all participants and plotted against their respective location for M1 and S1. Note that the automatic peak selection it not constrained by number of peaks. Thus, there can be multiple peaks per brain area. Also, note the different scaling of the x-axis for M1 and S1. Despite small deviations (arrows in scatter plots) we can consistently see small, repeating, and mirrored representations in M1 and a single large linear representations in S1. Error bars refer to the standard deviation across participants.

medial-lateral axis in both the primary motor and primary sensory cortex. Columnar profiles along the central sulcus are shown in Fig. 3. In the primary motor cortex, we find a sharp switch in preference between grasping and retraction at a certain point along this axis (Fig. 3A left, echoing results shown in the last row of Fig. 2). In the primary sensory cortex, we find a strong preference to grasping tasks only. There are no clear areas that have a stronger S1 response to retraction versus grasping (Fig. 3A, right). This is likely because common grasping actions are more often associated with stimulations of the sensory receptors (exteroception on the fingertips and inside of the hand) compared to retraction actions. Representations of sensory proprioception in the primary sensory cortex might be similarly engaged for grasping and retraction movements and, thus, do not introduce a preference to either of the two motor actions in the sensory cortex. The columnar profiles in Fig. 3B also clearly demonstrate the multiple mirrored finger representations in M1, versus the single linear representation in S1. Finally, we quantified relative finger preferences across both columnar and layer dimensions (Fig. 3C). We find that there is a more gradual transition between preferred fingers (i.e., more overlap across finger representations) in superficial layers (solid lines) than in deeper layers (dashed lines), where the transition is sharper. This result is also confirmed in resting-state data (Fig. S8).

Besides task-based topographical descriptions, we also characterized the topography of finger representations in resting state functional connectivity with the sensory cortex. The aim of these investigations was to confirm the multiple digit representations in the motor cortex on data that does not rely on a specific task design. As expected from the task-based data, we find the same multi-stripe patterns in the primary motor cortex for A) task-induced motor activity, B) resting-state seed-based correlation, and C) selected independent components of FSL-melodic ICA (Fig. 4). In all three cases, the two investigated fingers (index and little) are represented as two clear patches in the sensory cortex (red and blue arrows in bottom left of Fig. 4A–C). In the motor cortex, however, multiple red and blue patches can be identified. The resulting stripe-pattern of blue-red-blue is very similar for task and resting-state results (red and blue arrows in top right of Fig. 4A–C). We find that the digit representations in the sensory cortex have a stronger connectivity with the grasping patches in the motor cortex compared to its retraction patches (Fig. 4E–D). This is consistent with the task results showing that the sensory cortex has stronger activity for grasping motor actions compared to retraction motor actions.

4. Discussion

The general topography of the cerebral cortex is that *similar tasks are processed next to each other*. This topography principle discriminates different domains in different brain areas and also nicely explains many topographic maps within brain areas. As for instance, in the early visual system, the main topographic organizational principle is the retinotopic alignment of eccentricity and polar angles. However, because the cortex is merely a two-dimensional sheet, any task with a multi-dimensional parameter space needs to be reduced to two dimensions and integrated into the large scale topology. As such, the early visual cortex not only represents eccentricity and polar angle, but also represents orientation and color preferences, binocular eye-preference, and flickering frequency preference. These multi-dimensional parameters are not mainly represented as large scale topographic maps, but their representations are instead collapsed onto the two-dimensional space of the cortical sheet and are topographically organized as microscopic columnar and hyper columnar patches at the scale of 0.3–1.0 mm.

In the context of the multi-dimensional task parameter space of the motor cortex, the situation is complicated by the combined representation of body part preferences, action preferences, flexion vs. extension movements, movement directions, muscle tone, planning, sequencing, etc. This parameter space of the primary motor cortex has been extensively studied with cytoarchitecture, using invasive electrophysiology and neuroimaging in animals. Graziano and Aflalo (2007a; 2007b) developed a model of a lateral primate motor cortex, how the dimensionality reduction can be mapped on a simulated cortical sheet, which matches the experimental results with surprising detail. Here, using high-resolution CBV-fMRI neuroimaging and topographical analysis tools, we investigate the organizational principles of the multidimensional parameter space of the motor cortex in humans. We show how different organizational principles of somatotopy and action maps are integrated across cortical columns and layers. And we characterise the spatial scale of somatotopic finger maps in humans. We find evidence for action specific representations of fingers in M1, as well as for finger specific representations. Our results reveal how these multiple organizational principles are combined in M1: We find multiple mirrored representations of individual fingers that are differently engaged for specific movement actions (Figs. 1–3). Thus, M1 is organized as an action map as well as a topographical finger map in small (0.9–1.2 mm) representations along the columnar dimension within 4–9 mm action patches.

The multiple representations of individual fingers can be seen in both, task-based fMRI and resting-state functional connectivity with S1 (Fig. 3). We find that the finger representations in the motor cortex are very similar across cortical depths. There are only small differences between superficial cortico-cortical input layers II/III and corticospinal output layers Vb/VI. Namely, the size of the finger representations is slightly smaller in deeper layers compared to superficial layers. One potential origin of the sharper body part representation in deeper layers might be associated with previously described phenomena of surround inhibition in M1 (Beck and Hallett, 2011).

As opposed to previous columnar fMRI studies, we do not only try to depict known structures with known shape and size as proof-of-principle for a method as previous studies. Instead here, we are finding previously unknown organization principles of sub-millimeter representations in M1. This is a fundamentally new approach and a paradigm shift for the field of *columnar* and *laminar* fMRI.

In the primary somatosensory cortex, we find no deviations from the homunculus model as shown previously in humans (Olman et al., 2012; Schellekens et al., 2018; Kolasinski et al., 2016; Schluppeck et al., 2018).

Previous digit mapping studies using GE-BOLD fMRI could not clearly identify the mirrored finger representation in the primary motor cortex. This might be due to the fact that GE-BOLD fMRI suffers from poor localization specificity due to the presence of large draining veins

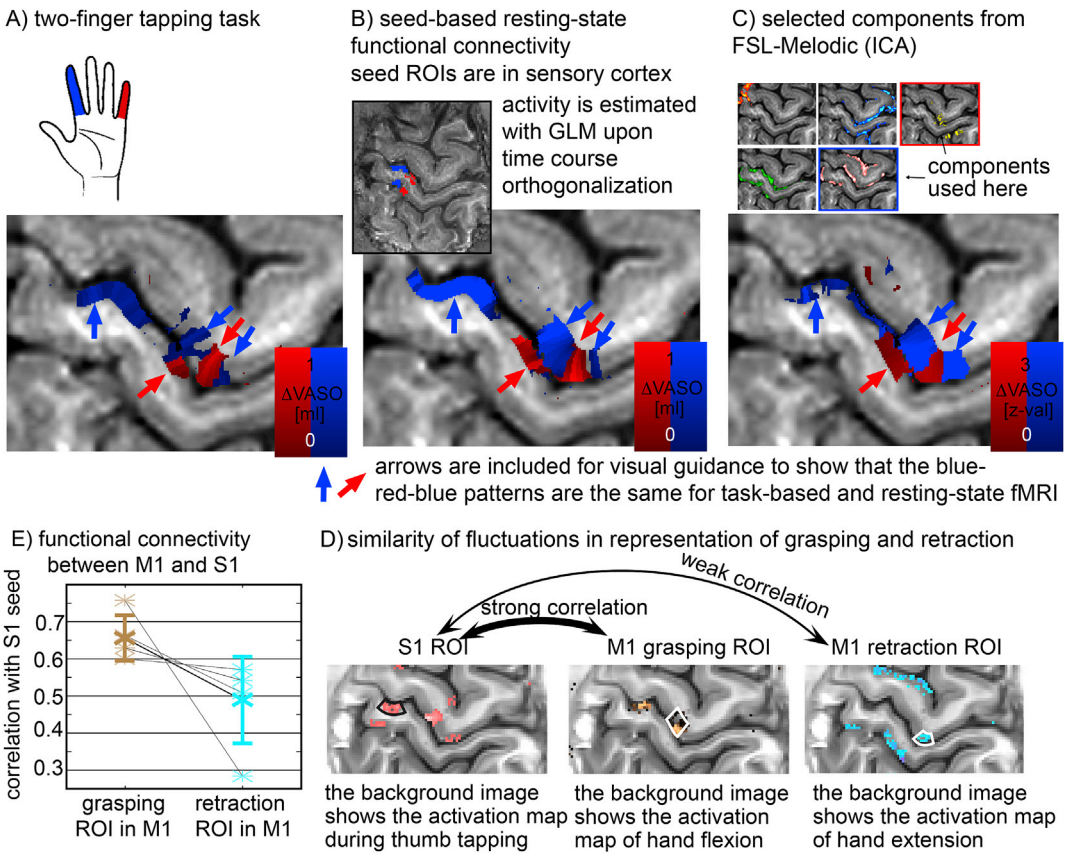

Fig. 4. Patterns of similar temporal fluctuations in resting-state activity match the patterns of task-evoked activity. A) Map of voxel wise preferences to become active during index finger movement or little finger movement. As shown in Figs. 1 and 2, the primary motor cortex has multiple representations of individual fingers. B) Map of resting-state signal fluctuation similarity for seed regions in the primary sensory cortex (inset). The colors refer to seed regions of interest (ROIs) that represent the little finger and index finger in S1. C) Very similar networks are generated using selected components from an ICA decomposition as seeds for connectivity analysis. Here we selected two (the ones outlined in blue and red) and used those as "seeds" to compute a preferential correlation map. D) The functional resting-state connectivity between individual finger representation areas in M1 and S1 are stronger for regions that represent grasping actions than for regions that represent retracting actions. E) Seed-based correlation analysis between the thumb representation in S1 and two thumb representations in M1 reveal that the flexion representation has larger functional connectivity to S1 than the extension representation. This might be associated with the fact that common grasping actions are more often associated with stimulations of the sensory receptors (on the inside of the hand) than retraction actions. The star symbols refer to individual participant and the error bars refer to the inter-participant standard deviation.

(Turner, 2002; Menon, 2002; Kim and Ogawa, 2012; Kennerley et al., 2005). Most human fMRI studies that investigated somatotopic organization likely did not have the sub-millimeter specificity to investigate deviations from the linear representation without methodological challenges (Siero et al., 2014; Olman et al., 2012; Schellekens et al., 2018; Hlustik et al., 2001; Dechent and Frahm, 2003). We believe the columnar specificity of GE-BOLD could be limited by two potential sources of venous contaminations. First, large principal veins are described to have tangential branch lengths of 2–6 mm (Fig. S8E (Duvernoy, 1981),). Thus, these tangential veins can result in more tangential signal mixing of GE-BOLD signal compared to their respective neural representations. Second, in some participants the sensory and motor banks of the central sulcus can be drained by the same pial veins. BOLD signal changes in the precentral gyrus can thus be contaminated by signal leakage from the postcentral gyrus. Other methodological challenges to identify the double-hand signature may arise from sensitivity limitations, task design, analysis design and effective resolution. Our results show that CBV-based fMRI has a higher localization specificity than conventional GE-BOLD fMRI (Figs. S2 and S5), thus overcoming the specificity limitations of previous studies. Even though CBV-based fMRI has a lower sensitivity and requires longer scan durations to exceed the detection threshold, it provides clearer results. The higher localization specificity of CBV-fMRI has previously been shown in humans with VASO fMRI (Huber et al., 2017) across cortical layers. In this study we extend this finding and also show the higher localization specificity of VASO across cortical columns. Note that the CBV weighting in VASO has been extensively validated by comparisons with gold-standard methods in rats and monkeys across layer and columns (Huber et al., 2015, 2014b; c; Kennerley et al., 2013).

To optimally separate individual digit representations, we included long rest periods into the experiment and used a pseudo-random ordering of individual fingers. This is different to previously employed “phase-encoding” paradigms and it comes at the cost of less efficient task design, requiring longer scan durations. However, it can be more sensitive to detect deviations of continuous linearly aligned representations.

Previous studies with PET had shown multiple hand movement representations across both sub-areas of the primary motor cortex (Geyer et al., 1996), BA4a and BA4p, respectively. The mirrored double-hand representation shown here (Figs. 2 and 3) is located in the anterior side (BA4a) of the primary motor cortex, only. Thus, the hand representations in BA4p, as discussed in (Geyer et al., 1996) refers to yet another representation of the fingers. This is the evolutionarily younger part of M1 that is located deep in the central sulcus. In this part of M1, individual body parts are largely overlapping (probably to facilitate complex hand movement) and thus, in this part of the motor cortex finger dominance maps might be misleading ways of depicting the complex representation principle (Ejaz et al., 2015). We find that the finger

representation in BA4p is actually not completely separated from the one in BA4a. It is partly connected to the representation in BA4a and does not show a mirrored pattern (Fig. S9).

In this study, we show for the first time that individual fingers have multiple representations in a mirrored pattern along the lateral-medial axis of primary motor cortex, with each whole-hand instance corresponding to a distinct movements. This mirrored representation across grasping and retraction patches gives rise to neighboring representations for movement synergies (D'Avella and Bizzi, 2005). As already suggested by Penfield (Penfield and Boldrey, 1937), our data show that the Penfield homunculus model is an oversimplification. With high resolution fMRI, we can confirm deviations of the homunculus model in M1 at very high resolutions corresponding to small body parts. Our data agree with the hypothesis that in the submillimeter regime, the motor cortex is organized as an action map (Graziano, 2016).

The present data corroborate several findings from invasive electrophysiologic recordings and microstimulation experiments in rodents and monkeys, that have elucidated the organizational principle of M1, and extend those to the level of the human M1. The presented methodology allows noninvasive recording of mesoscale functional representations in human M1 that were previously inaccessible. This might help to further understand the blueprint of cortical control over movement dynamics and kinematics. Beyond that, functional imaging of M1 at the layer and columnar level may help to elucidate how aberrations in the organizational principle could lead to movement disorders with largely unknown pathophysiology, such as dystonia.

5. Summary

Here we used advanced non-invasive neuroimaging in humans to provide novel insights in the organisational principles of the primary motor and sensory cortices at the mesoscale. We demonstrate for the first time that individual fingers are represented multiple times in the primary motor cortex in a columnar fashion following a mirrored pattern, and these representations are differentially engaged during specific motor actions (i.e., grasping versus retraction movements). By using new imaging and analysis technology that bridges the gap between invasive electrophysiological recordings and non-invasive large coverage mesoscopic fMRI in humans, we resolve previous controversies of M1 representation principles as 'body map' at the macro-scale vs. 'action maps' at the micro-scale.

Data and software availability

All raw, anonymized MRI data of this study can be anonymously downloaded

(https://layerfmri.page.link/Topography_raw). Fully processed data of one participant can be downloaded (https://layerfmri.page.link/TopographyData).

All custom written analysis software (source code) and evaluation scripts are available on Github

(https://github.com/layerfMRI/Tolopoly_strips). The authors are happy to share the 3D-VASO MR sequence upon request via a SIEMENS C2P agreement. A complete list of scan parameters used in this study is available on Github (https://github.com/layerfMRI/Sequence_ Github/tree/master/Topology).

Author contribution

L.H., conducted the experiments. L.H., P.B. designed the tasks. L.H., E.F. designed the analysis. L.H., S.K., D.G. wrote the analysis code. B.P., L.H., D.I. designed the MR-sequence, D.H., M.B., N.P., S.M., J.G. provided advice on experimental design, sequence, analysis, and research direction. L.H. wrote the draft of the manuscript. All authors contributed to the study story line and edited the manuscript.

Acknowledgements

The research was supported by the NIMH Intramural Research Program (ZIA-MH002783). We thank Kenny Chung and Harry Hall for radiographic assistance. The study was approved under NIH Combined Neuroscience Institutional Review Board protocol 93-M-0170 (ClinicalTrials.gov identifier: NCT00001360). Laurentius Huber was funded form the NWO VENI project 016.Veni.198.032 for part of the study. Portions of this study used the high-performance computational capabilities of the Biowulf Linux cluster at the National Institutes of Health, Bethesda, MD (biowulf.nih.gov). We thank Mark Hallett for comments on the manuscript. Benedikt Poser is funded by NWO VIDI 016.Vidi.178.052 and NIH MH111444 NIMH (PI Feinberg). Sriranga Kashyap is funded by NIH MH111444 NIMH (PI Feinberg). Natalia Petridou received funding from the Netherlands Organization for Scientific Research VIDI (NWO) grant 13339 and the National Institute of Mental Health award number R01MH111417. We thank James Kolasinsky for discussions about intermediate results of this study and task design.

Appendix A. Supplementary data

Supplementary data to this article can be found online at https://doi.org/10.1016/j.neuroimage.2019.116463.

References

Barinaga, M., 1995. Remapping the motor cortex. Science 268, 1696–1698. https://doi.org/10.1126/science.7792588. ISSN 0036-8075, 1095-9203.

Beck, S., Hallett, M., 2011. Surround inhibition in the motor system. Exp. Brain Res. 210 (2), 165–172. https://doi.org/10.1007/s00221-011-2610-6. ISSN 00144819.

Chainay, H., Krainik, A., Tanguy, M.L., Gerardin, E., Le Bihan, D., Lehéricy, S., 2004. Foot, face and hand representation in the human supplementary motor area. Neuroreport 15 (5), 765–769. https://doi.org/10.1097/00001756-200404090-00005. ISSN 09594965.

De Martino, F., Moerel, M., Ugurbil, K., Goebel, R., Yacoub, E., Formisano, E., 2015. Frequency preference and attention effects across cortical depths in the human primary auditory cortex. Proc. Natl. Acad. Sci. 112 (52), 16036–16041. https://doi.org/10.1073/pnas.1507552112. ISSN 00278424.

Dechent, P., Frahm, J., 2003. Functional somatotopy of finger representations in human primary motor cortex. Hum. Brain Mapp. 18 (4), 272–283. https://doi.org/10.1002/hbm.10084. ISSN 10659471.

Duvernoy, H.M., 1981. Cortical blood vessels of the human brain. Brain Res. Bull. 7, 519–579.

D'Avella, A., Bizzi, E., 2005. Shared and specific muscle synergies in natural motor behaviors. Proc. Natl. Acad. Sci. 102 (8), 3076–3081. https://doi.org/10.1073/pnas.0500199102. ISSN 00278424.

Ejaz, N., Hamada, M., Diedrichsen, J., 2015. Hand use predicts the structure of representations in sensorimotor cortex. Nat. Neurosci. 18 (7), 1034–1040. https://doi.org/10.1038/nn.4038. ISSN 15461726.

Geyer, S., Ledberg, A., Schleicher, A., Kinomura, S., Schormann, T., Burgel, U., Klingberg, T., Larsson, J., Zilles, K., Roland, P.E., 1996. Two different areas within the primary motor cortex of man. Nature 382, 805–807.

Graziano, M.S.A., 2016. Ethological action maps: a paradigm shift for the motor cortex. Trends Cogn. Sci. 20 (2), 121–132. https://doi.org/10.1016/j.tics.2015.10.008. ISSN 1879307X.

Graziano, M.S., Aflalo, T.N., 2007a. Mapping behavioral repertoire onto the cortex. Neuron 56 (2), 239–251. https://doi.org/10.1016/j.neuron.2007.09.013. ISSN 08966273.

Graziano, M.S., Aflalo, T.N., 2007b. Rethinking cortical organization: moving away from discrete areas arranged in hierarchies. The Neuroscientist 13 (2), 138–147. https://doi.org/10.1177/1073858406295918. ISSN 10738584.

Graziano, M.S.A., Taylor, C.S., Moore, T., 2002. Complex movements evoked by microstimulation of precentral cortex. Neuron 34, 841–851. https://doi.org/10.1177/1354068817740757. ISSN 14603683.

Hlustik, P., Solodkin, A., Gullapalli, R.P., Noll, D.C., Small, S.L., 2001. Somatotopy in human primary motor and somatosensory hand representations revisited. Cerebr. Cortex 11 (4), 312–321. https://doi.org/10.1093/cercor/11.4.312. ISSN 14602199.

Hua, J., Jones, C.K., Qin, Q., Van Zijl, P.C., 2013. Implementation of vascular-space-occupancy MRI at 7T. Magn. Reson. Med. 69 (4), 1003–1013. https://doi.org/10.1002/mrm.24334. ISSN 07403194.

Huber, L., Ivanov, D., Krieger, S.N., Streicher, M.N., Mildner, T., Poser, B.A., Möller, H.E., Turner, R., 2014a. Slab-selective, BOLD-corrected VASO at 7 tesla provides measures of cerebral blood volume reactivity with high signal-to-noise ratio. Magn. Reson. Med. 72 (1), 137–148. https://doi.org/10.1002/mrm.24916. ISSN 15222594.

Huber, L., Goense, J., Kennerley, A.J., Ivanov, D., Krieger, S.N., Lepsien, J., Trampel, R., Turner, R., Möller, H.E., 2014b. Investigation of the neurovascular coupling in positive and negative BOLD responses in human brain at 7T. Neuroimage 97, 349–362. https://doi.org/10.1016/j.neuroimage.2014.04.022. ISSN 10959572.

Huber, L., Goense, J.B.M., Kennerley, A.J., Guidi, M., Trampel, R., Turner, R., Möller, H.E., 2014c. Micro and macrovascular contributions to layer-dependent blood volume fMRI: a multi-modal, multi-species comparison. Proc. Int. Soc. Mag. Reson. Med. 22, 2114. https://doi.org/10.1002/mrm.24985.

Huber, L., Goense, J., Kennerley, A.J., Trampel, R., Guidi, M., Reimer, E., Ivanov, D., Neef, N., Gauthier, C.J., Turner, R., Möller, H.E., 2015. Cortical lamina-dependent blood volume changes in human brain at 7T. Neuroimage 107, 23–33. https://doi.org/10.1016/j.neuroimage.2014.11.046. ISSN 10959572.

Huber, L., Handwerker, D.A., Jangraw, D.C., Chen, G., Hall, A., Stüber, C., Gonzalez-Castillo, J., Ivanov, D., Marrett, S., Guidi, M., Goense, J., Poser, B.A., Bandettini, P.A., 2017. High resolution CBV-fMRI allows mapping of laminar activity and connectivity of cortical input and output in human M1. Neuron 96 (6), 1253–1263. https://doi.org/10.1016/j.neuron.2017.11.005. ISSN 10974199.

Indovina, I., Sanes, J.N., 2001. On somatotopic representation centers for finger movements in human primary motor cortex and supplementary motor area. Neuroimage 13 (6), 1027–1034. https://doi.org/10.1006/nimg.2001.0776. ISSN 10538119.

Kennerley, A.J., Berwick, J., Martindale, J., Johnston, D., Papadakis, N., Mayhew, J.E., 2005. Concurrent fMRI and optical measures for the investigation of the hemodynamic response function. Magn. Reson. Med. 54 (2), 354–365. https://doi.org/10.1002/mrm.20511. ISSN 07403194.

Kennerley, A.J., Huber, L., Mildner, T., Mayhew, J.E., Turner, R., Möller, H.E., Berwick, J., 2013. Does VASO contrast really allow measurement of CBV at high field (7 T)? An in-vivo quantification using concurrent optical imaging spectroscopy. Proc. Int. Soc. Mag. Reson. Med. 21, 0757.

Kim, S.G., Ogawa, S., 2012. Biophysical and physiological origins of blood oxygenation level dependent fMRI signals. J. Cereb. Blood Flow Metab. 32 (7), 1188–1206. https://doi.org/10.1038/jcbfm.2012.23. ISSN 0271678X.

Kolasinski, J., Makin, T.R., Jbabdi, S., Clare, S., Stagg, C.J., Johansen-Berg, H., 2016. Investigating the stability of fine-grain digit somatotopy in individual human participants. J. Neurosci. 36 (4), 1113–1127. https://doi.org/10.1523/JNEUROSCI.1742-15.2016. ISSN 0270-6474.

Kwan, H.C., MacKay, W.A., Murphy, J.T., Wong, Y.C., 1978. Spatial organization of precentral cortex in awake primates. II. Motor outputs. J. Neurophysiol. 41 (5), 1120–1131. https://doi.org/10.1152/jn.1978.41.5.1120. ISSN 0022-3077.

Lemon, R., 1988. The output map of the primate motor cortex. Trends Neurosci. 11 (11), 501–506.

Lu, H., Golay, X., Pekar, J.J., van Zijl, P.C.M., aug 2003. Functional magnetic resonance imaging based on changes in vascular space occupancy. Magn. Reson. Med. 50, 263–274. https://doi.org/10.1002/mrm.10519. ISSN 0740-3194.

Meier, J.D., Aflalo, T.N., Kastner, S., Graziano, M.S.A., 2008. Complex organization of human primary motor cortex: a high-resolution fMRI study. J. Neurophysiol. 100 (4), 1800–1812. https://doi.org/10.1152/jn.90531.2008. ISSN 0022-3077.

Menon, R.S., 2002. Postacquisition suppression of large-vessel BOLD signals in high-resolution fMRI. Magn. Reson. Med. 47 (1), 1–9. https://doi.org/10.1002/mrm.10041. ISSN 07403194.

Olman, C.A., Pickett, K.A., Schallmo, M.P., Kimberley, T.J., 2012. Selective BOLD responses to individual finger movement measured with fMRI at 3T. Hum. Brain Mapp. 33 (7), 1594–1606. https://doi.org/10.1002/hbm.21310. ISSN 10659471.

Park, M.C., Belhaj-Saïf, A., Gordon, M., Cheney, P.D., 2001. Consistent features in the forelimb representation of primary motor cortex in rhesus macaques. J. Neurosci. 21 (8), 2784–2792. ISSN 1529-2401.

Penfield, W., Boldrey, E., 1937. Somatic motor and sensory representation in. Brain: J. Neurol. 60 (February), 389–443. https://doi.org/10.1093/brain/60.4.389. ISSN 0006-8950.

Polimeni, J.R., Fischl, B., Greve, D.N., Wald, L., NeuroImage, L., 2010. Laminar analysis of 7 TBOLD using an imposed spatial activation pattern in. Neuroimage 52 (4), 1334–1346. https://doi.org/10.1016/j.neuroimage.2010.05.005. ISSN 1053-8119.

Porter, R., Lemon, R.N., 1993. Corticospinal Function and Voluntary Movement. Oxford University Press.

Poser, B.A., Koopmans, P.J., Witzel, T., Wald, L.L., Barth, M., 2010. Three dimensional echoplanar imaging at 7 Tesla. Neuroimage 51 (1), 261–266. https://doi.org/10.1016/j.neuroimage.2010.01.108. ISSN 10538119.

Sanchez Panchuelo, R.M., Ackerley, R., Glover, P.M., Bowtell, R.W., Wessberg, J., Francis, S.T., McGlone, F., 2016. Mapping quantal touch using 7 tesla functional magnetic resonance imaging and single-unit intraneural microstimulation. eLife 5 (MAY2016), 1–19. https://doi.org/10.7554/eLife.12812. ISSN 2050084X.

Sanes, J., Thangaraj, V., Edelman, R., Warach, S., Donoghue, J., 1995. Shared neural substrates controlling hand movements in human motor cortex. Science 268, 1775–1777. https://doi.org/10.1126/science.7792606. ISSN 0036-8075.

Scheiber, M.H., Hibbard, L.S., 1993. How somatotopic is the hand area? Science 261 (July), 489–492.

Schellekens, W., Petridou, N., Ramsey, N.F., 2018. Detailed somatotopy in primary motor and somatosensory cortex revealed by Gaussian population receptive fields. Neuroimage 179 (June), 337–347. https://doi.org/10.1016/j.neuroimage.2018.06.062. ISSN 10959572.

Schieber, M.H., 2002. Motor cortex and the distributed anatomy of finger movements. Adv. Exp. Med. Biol. 411–416.

Schluppeck, D., Sanchez-Panchuelo, R.M., Francis, S.T., 2018. Exploring structure and function of sensory cortex with 7 T MRI. Neuroimage 164 (January), 10–17. https://doi.org/10.1016/j.neuroimage.2017.01.081. ISSN 10959572.

Siero, J.C.W., Hermes, D., Hoogduin, H., Luijten, P.R., Ramsey, N.F., Petridou, N., 2014. NeuroImage BOLD matches neuronal activity at the mm scale : a combined 7 T fMRI and ECoG study in human sensorimotor cortex. Neuroimage 101, 177–184. https://doi.org/10.1016/j.neuroimage.2014.07.002. ISSN 1053-8119.

Strick, P.L., Preston, J.B., 1982. Two representations of the hand in area 4 of a primate. I. Motor output organization. J. Neurophysiol. 48 (1), 139–149. https://doi.org/10.1152/jn.1982.48.1.139. ISSN 0022-3077.

Strother, L., Medendorp, W.P., Coros, A.M., Vilis, T., 2012. Double representation of the wrist and elbow in human motor cortex. Eur. J. Neurosci. 36 (9), 3291–3298. https://doi.org/10.1111/j.1460-9568.2012.08241.x. ISSN 0953816X.

Turner, R., 2002. How much codex can a vein drain? Downstream dilution of activation-related cerebral blood oxygenation changes. Neuroimage 16 (4), 1062–1067. https://doi.org/10.1006/nimg.2002.1082. ISSN 10538119.